THERMODYNAMICS OF ADSORPTION OF METHYL FORMATE ON METAL DOPANT/ACTIVE CARBON SYSTEMS

Muhammad AFZAL and Fazal MAHMOOD

Department of Chemistry,
Quaid-I-Azam University, Islamabad, Pakistan

Received November 20, 1991
Accepted July 21, 1992

It has been found that doping of active carbon with metals (Ni, Cu, Zn, Cd) decreases its surface area due to dispersion of metal resides on the surface. A detailed examination of nitrogen adsorption indicates differences in the mode of dispersion of metals on the surface of active carbon. The adsorbing behavior of metal doped carbon for methyl formate was also studied as a function of temperature. From adsorption data, thermodynamic parameters such as free energy, enthalpy and entropy of adsorption were calculated using virial isotherm expression and interpreted. Results show that metal dopant/active carbon systems are synergic, exhibiting greater adsorption affinity for methyl formate than the sum of its constituents.

Active carbons are porous carbonaceous material which differ substantially in their properties from other porous materials and so extensively applied in chemical industry[1-4]. Active carbons are generally efficient adsorbents and the purification of gases represent one of its most frequent applications. The activity of carbon depends on intrinsic properties of parent material, porosity, ash content and method of activation. The chemical properties of active carbon can be modified by the addition of metals which have profound effect on both the reactivity and selectivity of the surfaces in catalytic reaction[5,6]. The behaviour of active carbon supported metals as catalyst is well known but little data are available with respect to adsorption of organic vapors like methyl formate. Methyl formate is becoming increasingly by important as a starting material for the preparation of acetic acid[7], dimethylformamide[8] and ethylene glycol[9].

EXPERIMENTAL

Active carbon was supplied by Merck (Catalog No. 2184). It was washed by several cycles of immersion in distilled water until there was no change in its pH. Metal(II) chlorides used were supplied by Merck with the purities better than 99%. Nitrogen gas used for adsorption experiments was 99.99% pure obtained from Masonlite (England) in break seal storage bulb.

For doping of active carbon, a predetermined amount of metal chloride was magnetically stirred in 200 ml of distilled water and 10 g of active carbon was added to mixture until a slurry was formed which was then dried under vacuum at 263 K for three hours. The dried sample were then heated at 735 K for five

hours in nitrogen atmosphere. A blank carbon sample was also prepared by giving the same treatment except that distilled water was used in place of the metal chloride solution.

For measurement of metal concentration, 1 g of the sample was thoroughly stirred with hydrogen perchlorate solution for 4 h at room temperature. The total amount of the metal in the solution was then determined by atomic absorption spectroscopy (Zeiss, Model FMD 47).

Complete adsorption–desorption isotherms for nitrogen were measured at 77 K using a Quantasorb sorption system and surface area was calculated by the BET method. Pore size distribution was determined from desorption isotherms of nitrogen by the method of Dollimore and Heal[10].

TPR system used for reduction was similar to that described by Karim[11].

Diffraction patterns for carbon samples were obtained with a Philips PW 1050 diffractometer goniometer. The detector was xenon proportional counter linked to PW 4620 ratemeter and channel analyzer. The radiation was Nickel filtered Cu Kα (1.5418 Å) generated in a Philips PW 1130/80 operated 1.0° diverging and 0.1° receiving slits at a scan rate of 2 deg/min. The continuous traces of X-ray reflections were obtained from the flat surface of the carbon pellets, since this techniques was found to give more reproducible results than from powder samples.

Adsorption data for methyl formate were obtained using CAHN 1000 electrobalance attached to a vacuum line. Before adsorption measurement, sample was dehydrated at 450 K in the vacuum of 10^{-5} mbar for five hours to remove condensed and physical adsorbed water. Then 0.25 g of the adsorbent was taken in glazed silica crucible, and the crucible was placed in the weighing unit. Prior to pumping, the hang down tube was maintained at a fixed temperature using a thermostat (accuracy ± 0.1 °C). The entire system was evacuated for at least seven hours before taking adsorption data. Vapors of the adsorptive were admitted and equilibrium pressure was recorded using a mercury manometer with the aid of a cathetometer. Dissolved gases were removed from the adsorptive liquid by freeze-pump-thaw technique.

RESULTS AND DISCUSSION

Structure of Doped Active Carbon

The relationship between the surface area of active carbon and the concentration of the metal is given in Table I. It is evident that the BET surface area of active carbon decreases with the increasing amount of doped metal. It indicates that these metals do not contribute any extra surface area to the active carbon. Decrease in surface area with the increasing amount of the metal may be due to dispersion of metal resides on the surface of active carbon and different degree of dispersion reflect a property of the doped material itself.

The idea of the presence of metal resides on the surface of active carbon in dispersed forms is consistent with pore size distribution curves as shown in Fig. 1. These curves show that the number of micro pore with radii 11 Å for copper doped carbon are significantly smaller than that of parent active carbon. In contrast, the number of pores with radii larger than 11 Å are nearly identical to active carbon and it is true for all systems with a different extent. Decrease in microporosity supports the idea that the metal resides are present in dispersed forms and more preferentially exist at active carbon micropore entrance leading to an appreciable pore blockage as confirmed by TPR studies.

TABLE I

Adsorption data for metal doped carbons (M_{mt}^0 metal concentration in mol/100 g of carbon; M_{mt}^{sup}/M_{mt}^0 ratio of supported metal to charged metal; A_{sp}^{BET} BET surface area; c_{mt}^{sup} metal concentration per unit area; V_{sp}^{pore} total pore volume)

M_{mt}^0	M_{mt}^{sup}/M_{mt}^0	A_{sp}^{BET}, $m^2\ g^{-1}$	c_{mt}^{sup}, $g\ m^{-2}$	V_{sp}^{pore}, $cm^3\ g^{-1}$
		Carbon		
–	–	849.3	–	1.303
		Ni–C		
0.017	0.995	801.1	0.00051	1.161
0.035	0.993	793.2	0.00252	–
0.060	0.963	773.8	0.00419	0.909
0.080	0.911	754.7	0.00528	–
0.103	0.903	731.4	0.00675	0.728
		Cu–C		
0.0160	0.991	781.7	0.00124	1.171
0.0300	0.988	772.7	0.00233	–
0.0550	0.973	763.3	0.00420	0.885
0.0800	0.969	753.4	0.00609	0.741
0.0950	0.952	736.5	0.00710	–
		Zn–C		
0.0150	0.993	815.2	0.00120	–
0.0550	0.967	786.9	0.00429	0.812
0.0770	0.971	763.3	0.00604	0.712
0.0950	0.970	746.7	0.00744	0.963
		Cd–C		
0.0170	0.989	763.6	0.00233	1.153
0.0300	0.982	754.5	0.00409	0.923
0.0375	0.950	738.8	0.00494	–
0.0500	0.947	728.9	0.00657	–
0.0580	0.941	709.6	0.00758	0.717
0.0800	0.838	675.1	0.01042	0.695

TPR profiles for supported metals on high surface area active carbon (containing 5% (w/w) of metal) are given in Fig. 2. TPR profile for active carbon gives no reduction peak at 800 K and behave like inert material. A broad reduction peak was observed at 293 K but the hydrogen uptake is negligible indicating that it may be due to some impurities entrapped within the pores of active carbon. The TPR profile obtained for supported cadmium shows well defined one broad reduction peak centered at 592 K. The hydrogen consumed nearly corresponds to complete reduction of all the cadmium present which indicates that the reduction of Cd^{2+} takes place in single step. The reduction pattern characterized by a broad peak tailed towards higher temperature denote a slow reduction process. This may be because of the low nucleation rate of isolated and small metal cluster as reported by many other workers[12]. The TPR profile obtained for supported zinc also shows one broad reduction peak centered at 664 K. It is found that the value of T_{max} was lowered by 60 K to its bulk value with reduction profile somewhat broader. The broadness of the reduction peak could be explained in

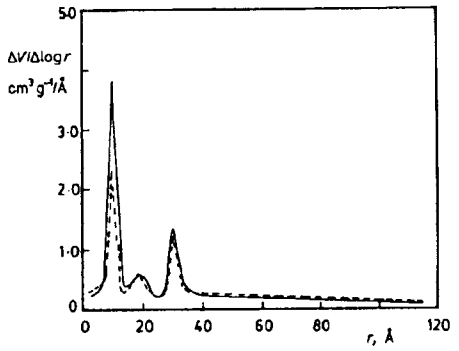

FIG. 1
Pore size distribution of active carbon (——) and metal doped active carbon (– – – –) containing 0.074 mol/100 gram of carbon

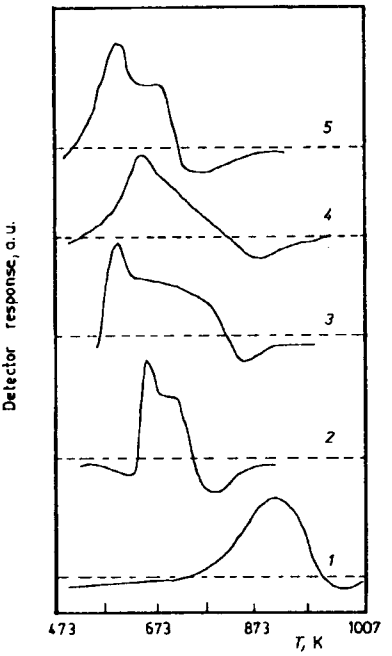

FIG. 2
TPR profiles for: *1* active carbon; *2* Cu–C; *3* Cd–C; *4* Zn–C; *5* Ni–C

terms of the heterogeneity of the systems in which supported metals are present in a dispersed phase rather than a stoichiometric compound. Active carbon in this case appears to act as a dispersing agent and promotes the reactivity of zinc towards reduction.

TPR profile for supported nickel shows two reduction peaks one at 621 K and other at 673 K. The low temperature reduction peak occur nearly the reduction temperature of supported nickel oxide. The second reduction at high temperature peak is from a specie which is more difficult to reduce. The TPR profile for supported copper shows a typical reduction at 668 K contributes more than 80% towards the total reduction. This indicates that support acts as dispersing agent and enhance the reduction of copper towards low temperature.

The high temperature reduction peaks observed is supported copper and nickel could be either due to surface–metal interactions or the presence of metals resides in two different pores of active carbon. The relation between low and high temperature reduction peaks with different pore sizes has been recently studied in detail by Brynmoore[13]. He observed that low temperature peaks are associated small pores and high temperature peak with the large pores. Similar TPR profiles has been reported by others but not discussed[14 - 16].

Thermodynamic Parameters of Methyl Formate Adsorption

Adsorption isotherm of methyl formate on active carbon and metal doped carbons (containing 0.07 mol of metal/100 gram of active carbon) were taken in the temperature range of 273 to 303 K. From adsorption data, thermodynamic parameters such as enthalpy, entropy and free energy of adsorption were calculated from virial isotherm

TABLE II
TPR measurements on active carbon and metal doped carbons

Adsorbent	Hydrogen uptake			Hydrogen desorption			Net M/H ratio
	T_{max}, K	$\nu(H)^a$	M/H	T_{min}, K	$\nu(H)^a$	M/H	
Carbon	922	49	–	997	39	–	–
Cu–C	668	651	1.67	708	72	0.092	1.59
Ni–C	621	736	1.73	723	82	0.096	1.63
Zn–C	664	623	1.63	908	101	0.132	1.49
Cd–C	592	402	1.81	816	49	0.108	1.70

[a] ν = μmol g^{-1}.

expression as approached by Anderson et al.[17]. The importance of this approach is that it allows to determine the thermodynamic parameters irrespective of the adsorbate–adsorbate interactions or the mechanism of adsorption.

The amount of adsorption c and the pressure p measured at different temperatures were introduced in virial expression

$$p = c / K \exp (2 A_1 c + 3/2 A_2 c^2 + 4/3 A_3 c^3 + 5/4 A_4 c^4 + \ldots), \qquad (1)$$

TABLE III
Values of virial coefficients A_1, A_2, A_3 and A_4 at different temperatures for active carbon and metal doped carbons

Adsorbent	T, K	A_1 [mol dm^{-3}]$^{-1}$	A_2 [mol dm^{-3}]$^{-2}$	A_3 [mol dm^{-3}]$^{-3}$	A_4 [mol dm^{-3}]$^{-4}$
Carbon	303	4.765	−35.290	70.822	−44.606
	293	5.371	−28.795	45.097	−22.672
	283	6.854	−34.940	51.991	−24.448
	273	9.555	−55.215	93.451	−49.136
Ni–C	303	4.271	−22.816	47.962	−32.712
	293	5.785	−29.185	57.932	−37.525
	283	7.351	−44.880	−65.872	−33.632
	273	7.580	−26.538	33.472	2.228
Cu–C	303	4.926	−23.304	39.847	−21.224
	293	6.225	−26.765	36.781	−16.072
	283	7.351	−26.466	34.410	4.3844
	273	7.580	−26.538	33.472	−13.752
Zn–C	303	6.030	−29.065	82.725	−53.928
	293	7.690	−19.653	38.325	−14.736
	283	13.59	−42.884	99.990	−50.672
	273	17.450	−75.504	114.001	−55.584
Cd–C	303	3.095	−12.665	20.947	−11.929
	293	6.522	−33.099	58.177	−32.536
	283	7.105	−28.624	36.815	−19.792
	273	10.001	−40.649	58.995	−27.664

where p is the pressure of adsorptive in atmosphere, c is the concentrations of the adsorbate in mol cm^{-3}, K is the thermodynamic equilibrium constant (mol dm^{-3} atm^{-1}) and A_1, A_2, A_3 and A_4 are virial coefficients.

Values of thermodynamic equilibrium constant were calculated by plotting $\ln (c/p)$ vs c. As $c \rightarrow 0$, $\ln (c/p) \rightarrow \ln K$; see Eq. (*1*).

From the values of thermodynamic equilibrium constant, thermodynamic parameters (ΔG^0, ΔH^0, ΔS^0) of adsorption were calculated by using the relation.

$$\Delta G^0 = RT \ln K \tag{2}$$

$$\Delta H^0 = RT^2 \, \mathrm{d}(\ln K)/\mathrm{d}T \tag{3}$$

$$\Delta S^0 = R \ln k + RT \, \mathrm{d}(\ln K)/\mathrm{d}T \tag{4}$$

The values of ΔG^0, (Fig. 3) are negative for all systems as expected for a spontaneous adsorption process. These values become more negative with the decrease of temperature indicating that these systems have high adsorption affinity for methyl formate at low temperature. The values of free energy of adsorption are higher for doped carbons that those for active carbon showing that adsorption of methyl formate is more favorable on metal doped carbons. This increase in adsorption is because of an increase in enthalpy of adsorption indicating strong adsorbate–adsorbent interactions while a decrease in entropy shows a cooperative effect between these two. Similar results are reported by Siedleswki et al.[18] who studied the adsorption of methanol on

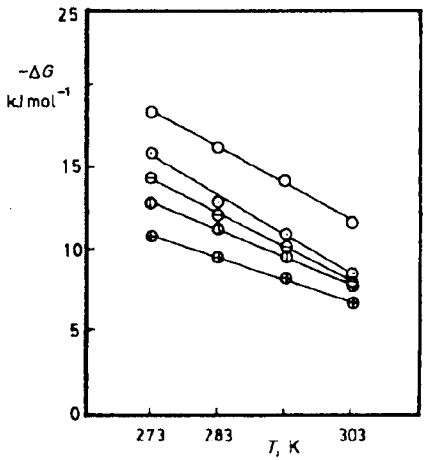

FIG. 3

Plots of variation of free energy of adsorption with temperature. Carbon (○), Ni–C (⊖), Cu–C (⊙), Zn–C (⊕) and Cd–C (⊗)

metal impregnated carbon and reported that methanol is adsorbed strongly on the metal sites present on the surface of carbon.

Figure 4 shows the relation between the values of enthalpy of adsorption and Pauling electronegativities of the metals. It indicates that enthalpy values increase with the increase in the electronegativities of the metals. It means that the reactivity of methyl formate towards metals differs, depending on the chemical nature of the metal and electronegativity of the metal may be one of them[19]. It might be assumed that adsorptive molecules are polar in nature, adsorb on metal sites due to inductive or specific interactions which may depend upon the electronegativity of metal.

TABLE IV
Adsorption enthalpy (ΔH) and entropy (ΔS) values in the temperature range of 273 – 303 K

Adsorbent	$-\Delta H$, kJ mol^{-1}	$-\Delta S$, J mol^{-1} K^{-1}
Carbon	42.15 ± 4.12	110.16 ± 10.08
Cu–C	113.77 ± 5.87	295.56 ± 28.90
Ni–C	84.06 ± 3.78	243.25 ± 22.98
Zn–C	76.91 ± 6.17	215.34 ± 30.41
Cd–C	59.56 ± 4.98	145.54 ± 15.67

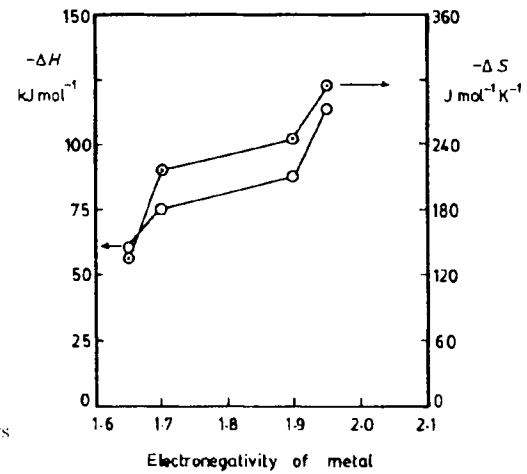

FIG. 4
Enthalpy (○) and entropy (⊖) of adsorption vs Pauling electronegativity of metal

REFERENCES

1. Ruthven D. M., Raghavan N. S., Hassan M. M.: Chem. Eng. Sci. *41*, 1325 (1986).
2. Hassan M. M., Raghavan N. S., Ruthven D. M.: Chem. Eng. Sci. *42*, 2037 (1987).
3. Grunewald G. C., Drago R. S.: J. Mol. Catal. *58*, 227 (1990).
4. Surinova S. I., Kostomarova M. A., Pethokov S. S.: Zh. Prikl. Khim. (Leningrad) *60*, 640 (1987).
5. Cilense M., Banadetti A. V., Jafelicci J. M., Varela J. A., DaCosta R. A.: Electrica Quim. *9*, 23 (1984).
6. Gerald G. C., Russel S. D.: J. Am. Chem. Soc. *113*, 1639 (1991).
7. Schreck D. J., Busby D. C., Wegman R. W.: J. Mol. Catal. *47*, 117 (1988).
8. Pruett R. L., Kaemarcik R. T.: Organometallics *1*, 1693 (1982).
9. Hratani T., Noziri S.: Chem. Econ. Eng. Rev. *17*, 21 (1985).
10. Dollimore D., Heal G. R.: J. Appl. Chem. (London) *14*, 109 (1964).
11. S. Karim: *Thesis*. Brunel University, Uxbridge 1991.
12. Delmon B., Houalla M. in: *Preparation of Catalysis II* (B. Delmon, P. Grange, P. A. Jacobs and G. Poncelet, Eds), p. 439. Elsevier, Amsterdam 1979.
13. Brynmoore M.: J. Catal. *114*, 217 (1988).
14. Taylor W. F., Yates D. J. C., Simflet J. H.: J. Phys. Chem. *68*, 2962 (1964).
15. Roberts S. D., McNeil B. D., DeBoss J. H., Kloet S. C.: J. Catal. *37*, 424 (1975).
16. Unmuth E. E., Schwartz C. H., Butt J. B.: J. Catal. *61*, 242 (1980).
17. Anderson M. W., Klinowski J.: J. Chem. Soc., Faraday Trans. 1 *82*, 3569 (1986).
18. Sidlewski J., Rychliki G.: Przem. Chem. *54*, 334 (1975).
19. Sexton B. A., Hughes A. E.: Surf. Sci. *140*, 227 (1984).